2008

Inverse Wavelet Reconstruction for Resolving the Gibbs Phenomenon

Nataniel Greene
CUNY Kingsborough Community College

Recommended Citation

N. Greene, "Inverse Wavelet Reconstruction for Resolving the Gibbs Phenomenon," International Journal of Circuits, Systems and Signal Processing, Vol. 2, Issue 2, 2008, pp. 73-77.

INTERNATIONAL JOURNAL of CIRCUITS, SYSTEMS and SIGNAL PROCESSING
Issue 2, Volume 2, 2008

Inverse Wavelet Reconstruction for Resolving the Gibbs Phenomenon

Nataniel Greene

***Abstract*— The Gibbs phenomenon refers to the lack of uniform convergence which occurs in many orthogonal basis approximations to piecewise smooth functions. This lack of uniform convergence manifests itself in spurious oscillations near the points of discontinuity and a low order of convergence away from the discontinuities. Here we describe a numerical procedure for overcoming the Gibbs phenomenon called the inverse wavelet reconstruction method. The method takes the Fourier coefficients of an oscillatory partial sum and uses them to construct the wavelet coefficients of a non-oscillatory wavelet series.**

***Index Terms*— Gibbs phenomenon, Inverse wavelet reconstruction, Inverse polynomial reconstruction.**

Fourier and orthogonal polynomial series are known for their highly accurate expansions for smooth functions. In fact it is known that the more derivatives a function has, the faster the approximation will converge. However, when a function possesses jump-discontinuities the approximation will fail to converge uniformly. In addition, spurious oscillations will cause a loss of accuracy throughout the entire domain. This lack of uniform convergence is known as the Gibbs phenomenon. Methods for post-processing approximations which suffer from the Gibbs phenomenon include the Gegenbauer reconstruction method of Gottlieb and Shu [7,9], the method of Pade approximants due to Driscoll and Fornberg [2], the method of spectral mollifiers due to Gottlieb and Tadmor [8] and Tadmor and Tanner [18, 19], the inverse polynomial reconstruction method of Shizgal and Jung [13,14,15,16,17], and the Freund polynomial reconstruction method of Gelb and Tanner [6]. These reconstruction methods can be combined with an effective method for edge-detection developed by Gelb and Tadmor [3,4,5,6], to yield an exponentially accurate reconstruction of the original function. In this paper we describe a new numerical method for overcoming the Gibbs phenomenon following the work of Shizgal and Jung, called the Inverse Wavelet Reconstruction method.

We begin with a brief review of the essential definitions of wavelets which we will need. Recall that a wavelet is a function $\psi \in L^2(\mathbf{R})$ satisfying:

$$\int_{-\infty}^{\infty} \psi(x)\, dx = 0 \tag{1}$$

This work was supported in part by a PSC-CUNY Research Award (grant No. 60106-35 36).

N. Greene is with the City Univeristy of New York, Department of Mathematics and Computer Science, Kingsborough Community College, 2001 Oriental Boulevard, Brooklyn, NY 11235 USA (e-mail: ngreene.math@gmail.com).

and

$$\int_{-\infty}^{\infty} \frac{\left|\widehat{\psi}(\xi)\right|}{|\xi|} d\xi < \infty, \tag{2}$$

where $\widehat{\psi}$ here is the Fourier transform of ψ. The function ψ is also known as an analyzing wavelet or a mother wavelet since any function $f \in L^2(\mathbf{R})$ can be expressed as a continuous sum of translations and dilations involving ψ according to the continuous wavelet transform. The continuous wavelet transform is given by

$$(W_\psi f)(b,a) = |a|^{-1/2} \int_{-\infty}^{\infty} f(t)\, \overline{\psi\left(\frac{t-b}{a}\right)} dt$$

and the inverse continuous wavelet transform is given by

$$f(x) = \frac{1}{C_\psi} \int_{-\infty}^{\infty} \int_{-\infty}^{\infty} \left[(W_\psi f)(b,a)\right] \frac{\psi_{b,a}(t)}{a^2} da db \tag{3}$$

where

$$\psi_{b,a}(t) = |a|^{-1/2}\, \overline{\psi\left(\frac{t-b}{a}\right)}$$

and

$$C_\psi = \int_{-\infty}^{\infty} \frac{\left|\widehat{\psi}(\xi)\right|}{|\xi|} d\xi.$$

A discrete wavelet series is given for fixed constants a_0, b_0 by

$$f(x) = \sum_{j=-\infty}^{\infty} \sum_{k=-\infty}^{\infty} c_{j,k} \psi_{j,k}(x) \tag{4}$$

where the discrete wavelet series coefficients are given by

$$c_{j,k} = (W_\psi f)\left(\frac{b_0 k}{a_0^j}, \frac{1}{a_0^j}\right)$$

and

$$\psi_{j,k}(x) = a_0^{j/2} \psi\left(a_0^j x - b_0 k\right).$$

In general the wavelet functions $\psi_{j,k}$ do not constitute an orthonormal basis. Instead they constitute what is known as a frame. The family of functions $\psi_{j,k}$ is a frame if

$$A\|f\|^2 \le \sum_{j=-\infty}^{\infty} \sum_{k=-\infty}^{\infty} \left|\langle f, \psi_{j,k}\rangle\right| \le B\|f\|^2$$

for positive constants A and B. When $A = B$ the functions $\psi_{j,k}$ are known as a tight frame. For more information see Daubechies [1]. The inverse wavelet reconstruction method makes use of wavelet bases and frames.

 Manuscript Received May 2, 2008; Revised received July 30, 2008

I. The Inverse Wavelet Reconstruction Method

A. Inverse Polynomial Reconstruction

An effective technique for dealing with the problem of the Gibbs phenomenon is the inverse polynomial reconstruction method of Shizgal and Jung. Their inverse method is itself an alternative approach to the original direct Gegenbauer reconstruction method of Gottlieb and Shu [7, 9]. In the inverse method, one solves a system of linear equations for the Gegenbauer polynomial reconstruction coefficients in terms of the given Fourier coefficients, from an expansion which suffers from the Gibbs phenomenon. The inverse polynomial reconstruction method begins with a Fourier partial sum

$$S_N f(x) = \sum_{n=-N}^{N} \widehat{f}(n)\, e^{-i\pi nx}. \tag{5}$$

The function also has a Gegenbauer-λ expansion given by

$$f(x) = \sum_{m=0}^{\infty} \widehat{f^{\lambda}}(m)\, C_m^{\lambda}(x)$$

where

$$\widehat{f^{\lambda}}(m) = \frac{1}{h_m^{\lambda}} \int_{-1}^{1} f(x)\, C_m^{\lambda}(x) \left(1-x^2\right)^{\lambda-1/2} dx \tag{6}$$

and

$$h_m^{\lambda} = \pi^{1/2} \frac{\Gamma(m+2\lambda)}{m!\Gamma(2\lambda)} \frac{\Gamma\left(\lambda+\frac{1}{2}\right)}{\Gamma(\lambda)(m+\lambda)}.$$

The Fourier coefficients $\widehat{f}(n)$ can be expressed in terms of Gegenbauer-λ coefficients as follows.

$$\begin{aligned}
\widehat{f}(n) &= \frac{1}{2}\int_{-1}^{1} f(x)\, e^{-i\pi nx} dx \\
&= \frac{1}{2}\int_{-1}^{1} \sum_{m=0}^{\infty} \widehat{f^{\lambda}}(m)\, C_m^{\lambda}(x)\, e^{-i\pi nx} dx \\
&= \sum_{m=0}^{\infty} \widehat{f^{\lambda}}(m) \left(\frac{1}{2}\int_{-1}^{1} C_m^{\lambda}(x)\, e^{-i\pi nx} dx\right) \\
&= \sum_{m=0}^{\infty} \widehat{f^{\lambda}}(m)\, c_{m,n}^{\lambda}
\end{aligned} \tag{7}$$

The connection coefficients $c_{m,n}^{\lambda}$ are given by

$$c_{m,n}^{\lambda} = \frac{1}{2}\int_{-1}^{1} C_m^{\lambda}(x)\, e^{-i\pi nx} dx \tag{8}$$

and can be computed numerically. An explicit formula for $c_{m,n}^{\lambda}$ was derived by this author, a form of which appeared in Greene [10], and is given by:

$$\begin{aligned}
c_{m,n}^{\lambda} &= \sum_{j=0}^{[m/2]} \frac{(-i)^{m-2j}}{\sqrt{2n}} J_{m-2j+\frac{1}{2}}(\pi n) \\
&\quad \times \frac{\left(\lambda-\frac{1}{2}\right)_j (\lambda)_{m-j} \left(\frac{3}{2}\right)_{m-2j}}{j!\left(\frac{3}{2}\right)_{m-j}\left(\frac{1}{2}\right)_{m-2j}},\ n \neq 0
\end{aligned} \tag{9}$$

$$c_{m,0}^{\lambda} = \begin{cases} \frac{\left(\lambda-\frac{1}{2}\right)_{m/2}(\lambda)_{m/2}}{j!\left(\frac{3}{2}\right)_{m/2}}, & m \text{ even} \\ 0, & m \text{ odd.} \end{cases} \tag{10}$$

The inverse polynomial reconstruction procedure is obtained by truncating the infinite series above and solving the system of equations

$$\widehat{f}(n) = \sum_{m=0}^{2N} \widehat{f^{\lambda}}(m)\, c_{m,n}^{\lambda},\ n = -N...N. \tag{11}$$

One then computes the reconstruction approximation

$$S_{2N}^{\lambda} f(x) = \sum_{m=0}^{2N} \widehat{f^{\lambda}}(m)\, C_m^{\lambda}(x). \tag{12}$$

The authors show that this final polynomial approximation does not depend on the choice of λ.

B. Inverse Wavelet Reconstruction

We explore here an analogous approach which seeks to reconstruct the original function in terms of wavelets. We begin with a Fourier partial sum as before and assume that the function $f(x)$ can also be expressed as a discrete wavelet series:

$$f(x) = \sum_{m=-\infty}^{\infty} \sum_{l=-\infty}^{\infty} c_{m,l} \psi_{m,l}(x)$$

where

$$c_{m,l} = \int_{-\infty}^{\infty} f(x)\, \overline{\psi_{m,l}(x)} dx$$

and

$$\psi_{m,l}(x) = a_0^{-m/2} \psi\left(a_0^m x - b_0 l\right).$$

We now derive a formula expressing the Fourier coefficients in terms of wavelet coefficients.

$$\begin{aligned}
\widehat{f}(n) &= \frac{1}{2}\int_{-1}^{1} f(x)\, e^{-i\pi nx} dx \\
&= \frac{1}{2}\int_{-1}^{1} \sum_{m=-\infty}^{\infty} \sum_{l=-\infty}^{\infty} c_{m,l} \psi_{m,l}(x)\, e^{-i\pi nx} dx \\
&= \sum_{m=-\infty}^{\infty} \sum_{l=-\infty}^{\infty} c_{m,l} \left(\frac{1}{2}\int_{-1}^{1} \psi_{m,l}(x)\, e^{-i\pi nx} dx\right) \\
&= \sum_{m=-\infty}^{\infty} \sum_{l=-\infty}^{\infty} c_{m,l} \widehat{\psi}_{m,l}(n)
\end{aligned} \tag{13}$$

The inverse wavelet reconstruction method is obtained by truncating the doubly infinite sum described above and solving for the wavelet coefficients. We suggest solving the following system of equations.

$$\widehat{f}(n) = \sum_{m=-M}^{M-1} \sum_{l=-L}^{L-1} c_{m,l} \widehat{\psi}_{m,l}(n) \tag{14}$$

where

$$n = -N...N-1, \text{and } N = 2ML \tag{15}$$

for the wavelet coefficients $c_{m,l}$. One then computes the wavelet reconstruction approximation

$$S_{M,L} f(x) = \sum_{m=-M}^{M-1} \sum_{l=-L}^{L-1} c_{m,l} \psi_{m,l}(x). \tag{16}$$

The terms $\widehat{\psi}_{m,l}(n)$ are the nth Fourier coefficients of $\psi_{m,l}(x)$. Since we are solving a system of $2N$ equations in $(2M)(2L) = 4ML$ unknown wavelet coefficients, in order for the system to be invertible we must have $2N = 4ML$ or $N = 2ML$. It is this convention which we will use for our numerical implementation below.

Numerical experiments indicate that the invertibility condition can be relaxed and fewer wavelet coefficients can be computed if one solves the overdetermined system in a least squares sense using Matlab's backslash operator. This is also illustrated below.

II. Numerical Results

Numerical experiments show that the inverse wavelet reconstruction approach does yield rapidly converging uniform approximations for a variety of wavelet families. We illustrate our method with several wavelet families. We use the Mexican hat wavelets [1] p. 75

$$\psi(x) = \frac{2}{\sqrt{3}\pi^{1/4}}\left(1-x^2\right)e^{-x^2/2}, \tag{17}$$

the Morlet wavelets [1] p. 76

$$\psi(x) = \cos(5x)\,e^{-x^2/2}, \tag{18}$$

the Poisson wavelets [12] p. 22

$$\psi(x) = \frac{1}{\pi\left(1+x^2\right)}, \tag{19}$$

and the second order Battle-Lemarie wavelets whose inverse Fourier transform is given by [1] pp. 146-148.

$$\begin{aligned}\widehat{\psi}(\xi) &= \sqrt{\frac{3}{2\pi}}e^{i\xi/2}\frac{\sin^4(\xi/4)}{(\xi/4)^2} \\ &\times\left(\frac{1+2\sin^4(\xi/4)}{\left(1+2\cos^2(\xi/2)\right)\left(1+2\cos^2(\xi/4)\right)}\right)^{1/2}.\end{aligned} \tag{20}$$

We consider the test functions $f_1(x) = \tan^{-1}(x)$, $f_2(x) = \sin(\cos(4x))$ and $f_3(x) = \cos(1.4\pi(x+1))$. The functions f_1 and f_3 both experience the Gibbs phenomenon at $x = \pm 1$. The function f_3 is naturally oscillatory and its inverse polynomial reconstruction was studied in [16]. The periodic extension of the function f_2 is continuous at $x = \pm 1$, however its first derivative is discontinuous resulting in a slowly converging Fourier series.

We implement the inverse wavelet reconstruction method by computing Fourier coefficients for the test functions in question using trapezoidal rule quadrature. This makes our Fourier series a pseudospectral series. For the method to be accurate we compute the coefficients $\widehat{\psi}_{m,l}(n)$ using the same trapezoidal rule quadrature. Results reported previously [11] were less accurate because they were implemented using Matlab's built in `quadl` function.

Rather than display semilogarithmic error plots for each choice of wavelet and each choice of the parameters a_0 and b_0, which would be cumbersome, we choose instead to display in the tables below the base 10 logarithm of the maximum absolute error of the reconstruction. This gives the order of the approximation in the uniform norm. To reflect the fact that the accuracy of the approximation throughout the interval is typically better than the maximum error, we also display the logarithm of the median absolute error.

No attempt has been made to optimize the parameters a_0 and b_0. There may be wavelet families as well as choices for a_0 and b_0 which significantly outperform the choices displayed here. Our goal has simply been to illustrate that the method works and yields highly accurate results.

In the tables below we consider 16, 36, 64, 100, and 144 Fourier coefficients and solve for an equal number of wavelet coefficients. The sequence is generated by setting $M = L$ so that the number of coefficients is given by $2N = 4M^2$ for $m = 2, 3, 4, 5$, and 6. It turns out that one need not be bound by this invertibility condition. The method is apparently stable when the number of Fourier coefficients is greater than the number of wavelet coefficients, when one solves the system in a least squares sense using Matlab's backslash operator. This is illustrated below where $20, 40, 80$ and 160 Fourier coefficients are taken and only 16, 36, 64, and 100 wavelet coefficients are computed.

$\log_{10}$ Maximum Absolute Error for $f_1(x)=\tan^{-1}(x)$					
Inverse Wavelet Reconstruction	**16**	**36**	**64**	**100**	**144**
Mexican Hat, a_0=2,b_0=1	-4.84	-8.9914	-10.9972	-10.9631	-12.588
Mexican Hat, a_0=2,b_0=0.25	-4.9156	-10.2833	-11.8902	-13.1775	-13.7196
Morlet, a_0=2,b_0=1	-3.9121	-8.7181	-11.2578	-11.0254	-13.1388
Morlet, a_0=2,b_0=0.25	-5.892	-9.1638	-12.004	-13.5823	-12.8753
Poisson, a_0=2,b_0=1	-3.2565	-5.7543	-7.3808	-7.5916	-8.6967
Poisson, a_0=2,b_0=0.25	-5.5509	-8.7931	-11.2796	-13.3344	-3.938
2nd Order Battle Lemarie, a_0=2,b_0=1	-3.8206	-10.1097	-11.9395	-11.8116	-12.293
Fourier pseudospectral series	0.1893	0.1931	0.1944	0.195	0.1954

A comparison of the maximum absolute error for several choices of wavelets illustrating apparent uniform convergence for $f_1(x)$.

$\log_{10}$ Median Absolute Error for $f_1(x)=\tan^{-1}(x)$					
Inverse Wavelet Reconstruction	**16**	**36**	**64**	**100**	**144**
Mexican Hat, a_0=2,b_0=1	-9.0001	-11.8381	-12.5455	-12.5417	-14.2855
Mexican Hat, a_0=2,b_0=0.25	-8.7112	-11.6824	-13.9538	-14.555	-14.5877
Morlet, a_0=2,b_0=1	-7.3297	-12.8633	-12.5719	-13.1682	-14.2033
Morlet, a_0=2,b_0=0.25	-9.3298	-12.9685	-14.774	-14.2578	-14.4954
Poisson, a_0=2,b_0=1	-7.2088	-9.2784	-9.2843	-9.6009	-9.7216
Poisson, a_0=2,b_0=0.25	-9.1974	-11.0949	-13.383	-14.5198	-14.5473
2nd Order Battle Lemarie, a_0=2,b_0=1	-7.5116	-14.1383	-14.5578	-14.1937	-14.2257
Fourier pseudospectral series	-1.4117	-1.7933	-2.0207	-2.4057	-2.4135

A comparison of the median absolute error for several choices of wavelets illustrating the typical error throughout the interval for $f_1(x)$.

$\log_{10}$ Maximum Absolute Error for $f_2(x)=\sin(\cos(4x))$					
Inverse Wavelet Reconstruction	**16**	**36**	**64**	**100**	**144**
Mexican Hat, a_0=2,b_0=1	0.9898	-2.3417	-5.976	-8.5293	-10.1221
Mexican Hat, a_0=2,b_0=0.25	0.7013	-2.6089	-6.0476	-7.6671	-9.0327
Morlet, a_0=2,b_0=1	-0.985	-4.0548	-5.859	-7.987	-10.0634
Morlet, a_0=2,b_0=0.25	0.0273	-3.1678	-6.3026	-8.8611	-9.8097
Poisson, a_0=2,b_0=1	-1.6189	-2.5051	-5.0994	-5.1191	-5.8211
Poisson, a_0=2,b_0=0.25	-0.8827	-4.3545	-6.9964	-7.1556	1.6162
2nd Order Battle Lemarie, a_0=2,b_0=1	-0.9911	-3.4192	-6.6519	-7.9922	-10.263
Fourier pseudospectral series	-1.2601	-1.6061	-1.9629	-3.9202	-2.5102

A comparison of the maximum absolute error for $f_2(x)$.

$\log_{10}$ Median Absolute Error for $f_2(x)=\sin(\cos(4x))$					
Inverse Wavelet Reconstruction	**16**	**36**	**64**	**100**	**144**
Mexican Hat, a_0=2,b_0=1	-3.2975	-5.564	-7.8135	-10.1354	-11.0672
Mexican Hat, a_0=2,b_0=0.25	-3.8393	-4.8392	-8.1026	-8.9621	-10.2115
Morlet, a_0=2,b_0=1	-3.8083	-7.3558	-8.5049	-10.1315	-11.4999
Morlet, a_0=2,b_0=0.25	-4.143	-7.0308	-8.5074	-9.7811	-11.0248
Poisson, a_0=2,b_0=1	-4.1257	-4.7126	-6.6713	-7.2824	-6.873
Poisson, a_0=2,b_0=0.25	-4.189	-7.1595	-7.3685	-8.7552	-8.8962
2nd Order Battle Lemarie, a_0=2,b_0=1	-4.2246	-8.1494	-8.8989	-10.3668	-11.6132
Fourier pseudospectral series	-2.1506	-2.8629	-3.3601	-3.9206	-4.0905

A comparison of the median absolute error for $f_2(x)$.

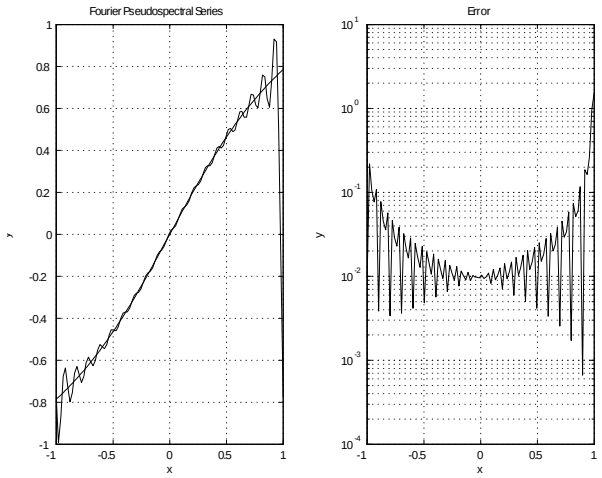

A 40 term pseudospectral Fourier series for $f_1(x) = \tan^{-1} x$.

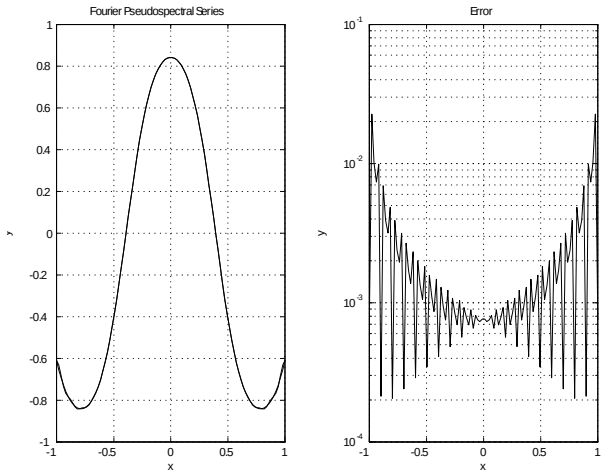

A 40 term pseudospectral Fourier series for $f_2(x) = \sin(\cos 4x)$.

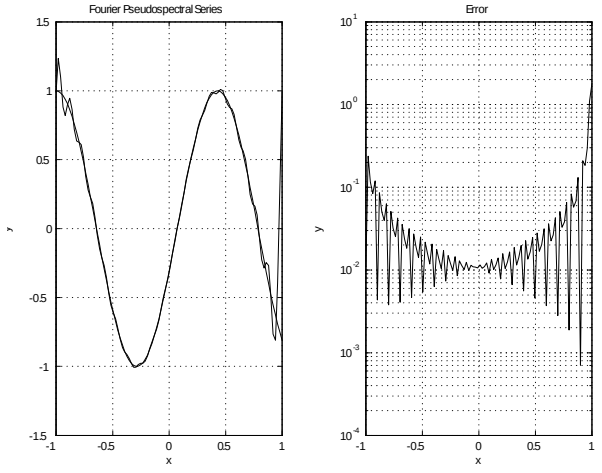

A 40 term pseudospectral Fourier series for $f_3(x) = \cos(1.4\pi(x+1))$.

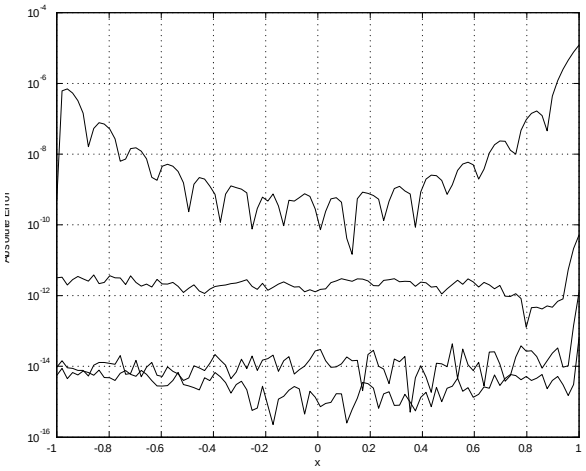

Absolute error for inverse Mexican Hat reconstruction of $f_1(x)$, $a_0 = 2, b_0 = 0.25$ from $16, 36, 64, 100$ Fourier coefficients using the same number of wavelet coefficients (the invertible case).

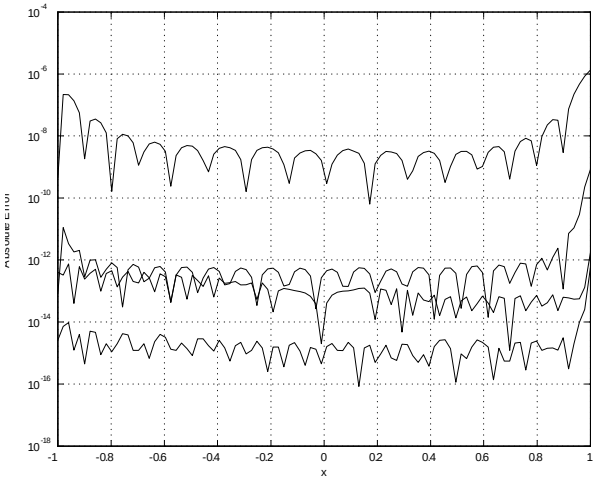

Absolute error for inverse Mexican Hat reconstruction of $f_1(x)$, $a_0 = 2$, $b_0 = 0.25$ from $20, 40, 80, 160$ Fourier coefficients using $16, 36, 64, 144$ wavelet coefficients respectively, solved in a least squares sense.

It is apparent that as the number of Fourier coefficients increases the error of the reconstruction initially decreases rapidly, but soon levels off at around 10^{-14} regardless of how many Fourier coefficients are used. This is due to the fact that the linear system is ill-conditioned and machine epsilon here is approximately 2.2×10^{-16}. All the wavelets shown perform comparably well, although some do slightly better than others. The results for the inverse wavelet reconstruction method in all cases appear comparable to the results reported for the inverse polynomial reconstruction method.

III. Conclusions and Future Work

Numerical results indicate that the inverse wavelet reconstruction method yields an accurate and uniformly converging reconstruction approximation for a variety of wavelets. Work in progress includes reconstruction involving the use of scaling

functions, reconstruction from series other than Fourier series, such as orthogonal polynomials or wavelets, a comparison with other methods, and a proof of convergence.

REFERENCES

[1] I. Daubechies, Ten Lectures on Wavelets, CBMS-NSF Regional Conference Series in Applied Mathematics, SIAM, Philadelphia, 1992.

[2] T. A. Driscoll, and B. Fornberg, A Pade-based Algorithm for Overcoming the Gibbs Phenomenon, *Numerical Algorithms,* 26, 2001, pp. 77-92.

[3] A. Gelb, and E. Tadmor, Detection of Edges in Spectral Data, *Appl. Comp. Harmonic Anal.*, 7, 1999, pp. 101-135.

[4] A. Gelb, and E. Tadmor, Detection of Edges in Spectral Data II. Nonlinear Enhancement, *SIAM J. Numer. Anal.*, Vol. 38, No. 4, 2000, pp. 1389-1408.

[5] A. Gelb, and E. Tadmor, Spectral Reconstruction of Piecewise Smooth Functions from their Discrete Data, *Mathematical Modeling and Numerical Analysis*, 36:2, 2002, pp. 155-175.

[6] A. Gelb, and J. Tanner, Robust Reprojection Methods for the Resolution of the Gibbs Phenomenon., *Applied Computational and Harmonic Analysis*, Vol. 20, 1, 2006, pp. 3-25.

[7] D. Gottlieb, C.-W. Shu, A. Solomonoff, and H. Vandeven, On the Gibbs's Phenomenon I: Recovering Exponential Accuracy from the Fourier Partial Sum of a Nonperiodic Analytic Function, *J. Comput. Appl. Math.*, 43, 1992, pp. 81-92 .

[8] D. Gottlieb, and E. Tadmor, Recovering Pointwise Values of Discontinuous Data within Spectral Accuracy, in: *Progress and Supercomputing in Computational Fluid Dynamics*, Proceedings of a 1984 U.S.-Israel Workshop, Progress in Scientific Computing, Vol. 6 (E. M. Murman and S. S. Abarbanel eds.), Birkhauser, Boston, 1985, pp. 357-375.

[9] D. Gottlieb and C.-W. Shu, On the Gibbs Phenomenon and its Resolution, *SIAM Rev.*, Vol. 39, 1997, pp. 644-668.

[10] N. Greene, *On the Recovery of Piecewise Smooth Functions from their Integral Transforms and Spectral Data*, Ph.D. Dissertation, SUNY Stony Brook, 2004.

[11] N. Greene, A Wavelet-based Method for Overcoming the Gibbs Phenomenon, in: *Proceedings of the American Conference on Applied Mathematics*, Cambridge, Massachusetts, March 24-26, 2008, pp. 408-412.

[12] M. Holschneider, Wavelets: An Analysis Tool, Oxford University Press, 1995.

[13] J.-H. Jung, and B. D. Shizgal, Generalization of the Inverse Polynomial Reconstruction Method in the Resolution of the Gibbs Phenomenon, *J. Comp. Appl. Math.*, v. 172, n.1, 2004, pp.131-151.

[14] J.-H. Jung, and B. D. Shizgal, Inverse polynomial reconstruction of two dimensional Fourier images, *J. Scientific Computing*, v.25, n.3, 2005, pp. 367-399.

[15] J.-H. Jung, and B. D. Shizgal, On the numerical convergence with the inverse polynomial reconstruction method for the resolution of the Gibbs phenomenon, *J. Computational Physics*, 224, 2007, pp. 477-488.

[16] B. D. Shizgal and J.-H. Jung, Towards the resolution of the Gibbs Phenomena, *J. Comput. Appl. Math.*, 16, 2003, pp. 41-65.

[17] R. Pasquetti, On Inverse methods for the Resolution of the Gibbs Phenomenon, *Journal of Computational and Applied Mathematics*, Vol. 170, no. 2, 2004, pp. 305-315.

[18] E. Tadmor and J. Tanner, Adaptive Mollifiers - High Resolution Recovery of Piecewise Smooth Data from its Spectral Information, *J. Foundations of Comp. Math.* 2, 2002, 155-189.

[19] E. Tadmor and J. Tanner, Adaptive Filters for Piecewise Smooth Spectral Data, *IMA J. Numerical Anal.*, Vol. 25, 4, 2005, pp. 635-647.